Scenario-based performance assessment of green-grey-blue infrastructure for flood-resilient spatial solution: A case study of Pazhou, Guangzhou, greater Bay area

Lu, P.; Sun, Yimin; Nijhuis, S.

DOI
10.1016/j.landurbplan.2023.104804

Publication date
2023

Document Version
Final published version

Published in
Landscape and Urban Planning

Citation (APA)
Lu, P., Sun, Y., & Nijhuis, S. (2023). Scenario-based performance assessment of green-grey-blue infrastructure for flood-resilient spatial solution: A case study of Pazhou, Guangzhou, greater Bay area. *Landscape and Urban Planning*, *238*(104804), Article 104804. https://doi.org/10.1016/j.landurbplan.2023.104804

Landscape and Urban Planning 238 (2023) 104804

Contents lists available at ScienceDirect

Landscape and Urban Planning

journal homepage: www.elsevier.com/locate/landurbplan

Scenario-based performance assessment of green-grey-blue infrastructure for flood-resilient spatial solution: A case study of Pazhou, Guangzhou, greater Bay area

Peijun Lu [a,b], Yimin Sun [a,*], Nijhuis Steffen [b]

[a] School of Architecture, State Key Laboratory of Subtropical Building Science, South China University of Technology, China
[b] Faculty of Architecture and the Built Environment, Department of Urbanism, Delft University of Technology, Netherlands

HIGHLIGHTS

- A scenario-based framework is proposed to rank infrastructure spatial designs.
- A coupled model assesses flood performance in spatiotemporal scales.
- A dynamic multi-criteria decision-making method considers temporal indicators.
- Waterway connectivity and green space redundancy improve flood resilience.
- Waterway storage improvement outperforms green space runoff reduction at source.

GRAPHICAL ABSTRACT

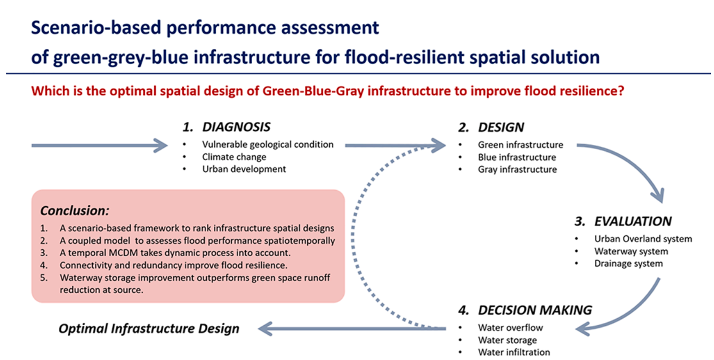

ARTICLE INFO

Keywords:
Flood resilience
Green-grey-blue infrastructure systems
Performance assessment
Inundation model
TOPSIS

ABSTRACT

Flood resilience has aroused significant interest in coastal areas dealing with a growing frequency of severe rainstorms caused by climate change and urbanisation. At the core of flood resilience is the development of a resilient green-grey-blue infrastructure system that can resist, absorb, and recover from floods in a timely manner. Current flood resilience research, however, is limited to evaluating single infrastructure systems, failing to examine the dynamic process or find ideal spatial infrastructure designs for decision-makers. This research proposes a scenario-based assessment framework for integrated green-grey-blue infrastructure systems to improve flood resilience during urban design decision-making. Rainfall-runoff, drainage networks, and river system models are interlinked to provide quantitative simulation evaluations of water quantity and urban impact in various spatial organisations of infrastructure design. A dynamic, multi-criteria decision-making process is used to reveal the importance of five temporal indicators and rank design alternatives. In Guangzhou, China, the efficiency of this architecture is demonstrated on Pazhou Island, a typical river network area. Given the limited water and green space available, the results demonstrate that submerged areas exert a greater influence during peak rainfall, and blue infrastructure storage becomes an essential factor following rainfall. Furthermore, from a spatial perspective, the looped network of green-blue infrastructure enhances flood resilience, and downstream waterway connections and green space-aligned waterways boost the water storage capacity of green-grey-blue

* Corresponding author.
E-mail addresses: scutlupj@gmail.com (P. Lu), arymsun@scut.edu.cn (Y. Sun), s.nijhuis@tudelft.nl (N. Steffen).

https://doi.org/10.1016/j.landurbplan.2023.104804
Received 25 July 2022; Received in revised form 5 May 2023; Accepted 12 May 2023

infrastructure. This paradigm can improve flood resilience in the Greater Bay Area in the future, especially in response to heavy rainstorms and river floods.

1. Introduction

Coastal flooding and urban inundation have had widespread and catastrophic impacts worldwide (Meyer & Nijhuis, 2013). China was the country most struck by natural hazard catastrophes from 2000 to 2019, with over 500 occurrences, most of which were hydrological and meteorological disasters (EM-DAT, 2019). Many cities in southern China, notably in the Greater Bay Area (GBA), have suffered flood catastrophes and intense rainstorms, resulting in significant socioeconomic damage (Chen, Li & Chen, 2021). In recent years, the flood resilience of infrastructure systems has garnered a lot of attention as a solution to address the difficulties of coastal flood management (Karamouz, Taheri, Khalili & Chen, 2019).

Traditional flood management focuses on grey infrastructures like drainage pipes, storm sewers, water pumps, and detention basins (Tavakol-Davani, Burian, Devkota & Apul, 2016). However, compared to green infrastructure (GI), grey infrastructure is more costly to maintain, less multifunctional, and vulnerable to damage when certain thresholds are exceeded during disaster events, which prevents them from adapting to climate change and changing social systems (Kuwae & Crooks, 2021). Low Impact Development (LID) deployment in GI is necessary to supplement traditional drainage systems. Integrating green and grey systems might provide catastrophe mitigation from a short-term perspective and ecological value and environmental benefit in the long run (Casal-Campos, Fu, Butler & Moore, 2015; Kuwae & Crooks, 2021). Novel approaches to attaining green-grey systems include Sponge City in China, Water Sensitive Urban Design in Australia, and the Sustainable Drainage System in the United Kingdom (Fletcher et al., 2015; Yin et al., 2022; Yin et al., 2021). According to some studies, combining storm water management models (SWMM) with multiple-objective optimisation approaches may result in cost-effective optimal solutions to minimise runoff and increase water quality (Leng, Chen, Zhu, Xu & Yu, 2021; Leng, Xu, Jia & Jia, 2022). Socioecological return and economic costs were also estimated through the life cycle assessment of green-grey infrastructures (Liu et al., 2021; Xu et al., 2021). However, past research has concentrated on the runoff phase of the decentralised GI at the source and the arrangement of LID. Related to flood occurrences, blue infrastructure (BI) and GI through flood-oriented terrain elevation modifications can be more efficient than runoff reduction at the source (Haghighatafshar et al., 2018). This encouraged us to demonstrate that the spatial structure of green–blue infrastructure (GBI) has evolved as a complement to the layout of LID (Chen et al., 2021; Leng et al., 2020).

Urban flood resilience describes a city's ability to resist, absorb, and recover from floods and to adapt and transform (Driessen et al., 2018). Unlike traditional urban flood management, urban flood resilience focuses on understanding and managing the dynamic character of urban water transitions (Johannessen & Wamsler, 2017). A typical green-grey-blue infrastructure system, which includes GI as redundancy space to absorb excess rainfall at the source, grey infrastructure to maintain the drainage and protection function at the midway, and BI to minimise and recover from the impact of extreme precipitation at the terminal, plays an essential role in improving urban flood resilience. Artificial pipe networks integrated with natural river networks constitute an efficient but vulnerable drainage system that constrains the adaptive capacity to environmental change in coastal areas, particularly flat locations with dense river networks. (Zhang, Wang, Li & Ding, 2017). GI, BI, and grey infrastructure should all be handled as part of a more comprehensive urban water management system (O'Donnell et al., 2020; Joyce, Chang, Harji & Ruppert, 2018). Assessing the effectiveness of urban flood resilience has been investigated recently (Bertilsson et al., 2019). However, the majority of present research focuses on the use of risk functions to predict the likelihood of urban flood impacts (Joyce, Chang, Harji & Ruppert, 2018) and the use of drainage system indicators (i.e., peak runoff) to assess the performance of BI and grey infrastructure (Yang & Best, 2015). Hereby, the relationship between the spatial structure of the infrastructure system and flood performance is not sufficiently evident, and the assessment indicators do not account for dynamic processes. Given the progress of hydrodynamic models and statistical techniques, it is time to examine the spatiotemporal flood performance of infrastructure systems and add dynamic indicators to the decision-making process.

Various software tools have been developed to predict flood impacts and the performance of water systems. Open-source tools, such as SWMM (Girona's, Roesner, Rossman & Davis, 2010) and Lisflood-FP (Neal et al., 2011), feature simple model development and high-performance computation but lack reliable coupling technology. Commercial tools packages like MIKE (Patro, Chatterjee, Mohanty, Singh & Raghuwanshi, 2009), Infoworks ICM (Sidek et al., 2021), and SOBEK Suite (Prinsen & Becker, 2011) feature a stable integrated platform and high accuracy. However, SOBEK Suite lacks the connection with SWMM, which is not ideal for analysing the effect of LID. In contrast, MIKE Suite provides a Python package which is convenient for processing simulation results automatically. Furthermore, the MIKE Suite has been extensively employed in the GBA, including Guangzhou (Liu, Cai, Wang, Lan & Wu, 2020), Shenzhen (Zhang et al., 2021), and Zhuhai (Yin et al., 2020). Selecting reliable, precise, and convenient software is essential to quantifying the flood resilience performance during rainstorms and river floods (Huang, Keisler & Linkov, 2011).

Various academics have utilised different statistical techniques to evaluate alternatives and choose the best design. Many studies employed multi-criteria decision-making (MCDM) strategies, which are used to resolve decision-making with high accuracy based on several decision criteria (Mulliner, Malys & Maliene, 2016). For urban flood control, several academics have created decision-making tools based on the MCDM approach (Mishra & Satapathy, 2020; Javari, Saghaei & Fadaei Jazi, 2021), and TOPSIS has been used to rank the options and choose the best option for improving flood resistance. Usually, MCDM deals with the criteria at a given point in time without considering their evolution over time, which can provide essential information (Campello, Duarte & Romanoa, 2022). Several MCDM methods, such as the temporal Vlse Kriterijumsk Optimizacija Kompromisno Resenje (VIKOR) and the dynamic Technique for Order Preference by Similarity to Ideal Solution (TOPSIS), have been used for sustainability assessment (Watróbski, Baczkiewicz, Ziemba & Sałabun, 2020; Li, Yi & Zhang, 2018). To evaluate the dynamic process of flood performance during rainfall, extending the temporal TOPSIS method is vital to generate a hierarchy of management decision options, which has been used extensively for environmental decision-making (Huang, Keisler & Linkov, 2011).

This research employs a typical river network region in Guangzhou, China, as a case study and offers an integrated scenario-based assessment framework to quantify and rank the resilience performance of various infrastructure spatial designs. It adopts an accurate, coupled hydrodynamic model to study the dynamic flood performance indicators in a green-grey-blue system. Five dynamic indicators (runoff reduction, water storage in BI, water storage in GI, overflow volume in roads, submerged area in development land) are selected to conduct a temporal MCDM utilising TOPSIS, enabling urban managers to fully grasp the performance of various interventions throughout the decision-making process. As a guide to strengthening flood resilience in practical projects, this scenario-based framework provides considerable quantitative information for decision-makers when choosing alternative designs.

2. Methods

An integrated scenario-based assessment framework will aid urban planners and designers in examining the performance of various spatial structures to choose the optimal infrastructure design to boost coastal flood resilience. However, typical performance evaluation approaches disregard the dynamic processes during extreme rainstorms and river floods. To solve this deficiency, this research presents a new paradigm for thoroughly examining flood resilience performance in support of green-grey-blue infrastructure systems for urban security. The main framework (Fig. 1) is divided into three sections: Part I is about spatial infrastructure design scenarios, Part II is about coupled hydrodynamic model simulation, and Part III is about temporal MCDM.

2.1. Spatial infrastructure design scenarios

2.1.1. Study area

The eastern part of Pazhou Island, in Guangzhou (23° 09′ N, 113° 39′ E), Guangdong Province, was utilised as the case study presented in this article. The region (Fig. 2) is the GBA's plain river network area. The eastern part of Pazhou Island has a total area of 5454 km^2 and is flanked by the Pearl River. This part is being developed as an economic centre to stimulate trade and entrepreneurship. Unfortunately, the region has been struck by extreme typhoons and heavy rains, such as Typhoon Mangkhut on Sept 16, 2018, and the extreme rainfall (181.1 mm) on May 7, 2017. Also, the existing mean height here is virtually equivalent to or even lower than the mean river water level. Therefore, strengthening flood protection in this region demands urgent urban infrastructure design.

2.1.2. Different spatial designs of the green-grey-blue infrastructure system

Various spatial designs of the green-grey-blue infrastructure system were designed given the limits of the area of water space (around 86.8 × 10^3 m^2) and green space (around 1.65 × $10^6 m^2$), the number of outlets, the cost of LID facilities (around 5.80 × 10^6 USD) (Table 1), the outdoor

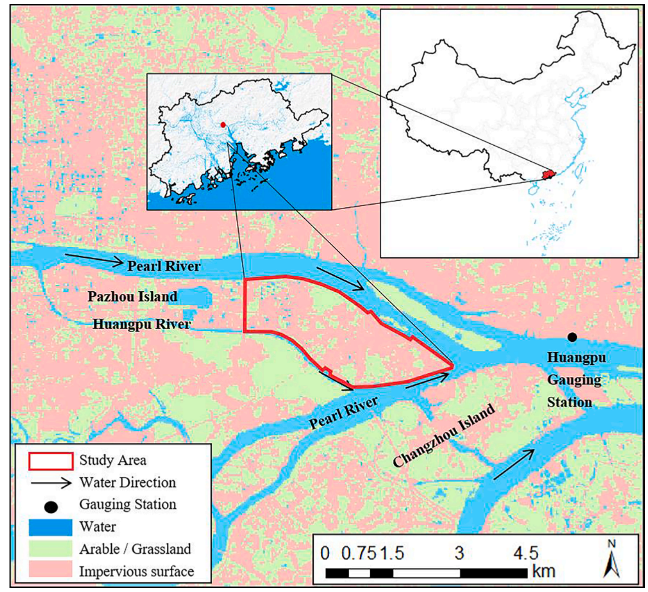

Fig. 2. The study area is in the eastern portion of Pazhou Island, centre of the GBA.

drainage design standards (GB50014-2021), and the land use and building footprints (Details see Supplementary material 1.5). The selection of LID facilities is generally based on "Technical Guidelines for Selection Method of Sponge City Low Impact Development Facilities" (CECS, 2021), taking runoff control goals, local design area features, and cost control targets into account. Green roofs (GR), permeable pavement (PP), and vegetable swales (VS) satisfied the criterion of spatial placement from the technical standards. The model's structural characteristics and cost of LID facilities are obtained from the User's Manual of SWMM and Guangzhou Sponge City Planning and Design Guidelines (Government, 2017). (Details see Supplementary material 1.4). The essential contrast distinction between the green and blue systems is their

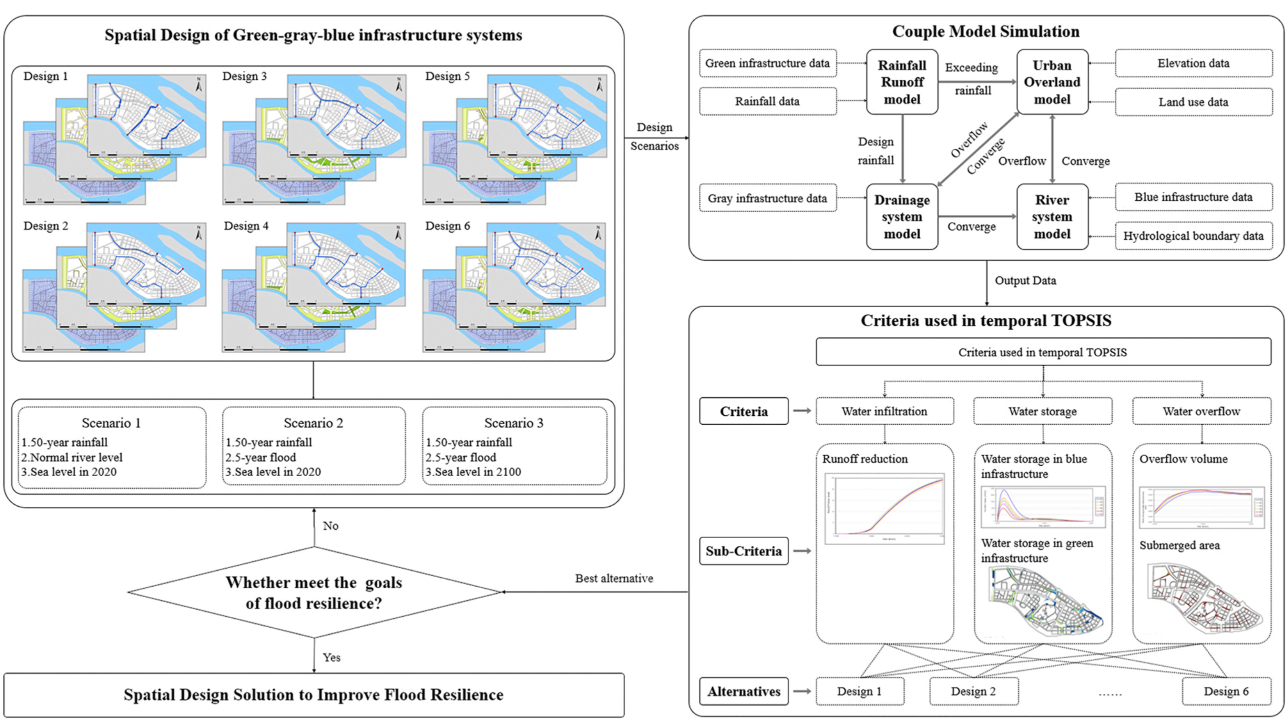

Fig. 1. The overall framework of scenario-based evaluation of green-grey-blue infrastructure for flood resilience.

Table 1
The statistic of GBI in different designs.

	D1	D2	D3	D4	D5	D6
Waterway length (km)	6.47	9.50	8.69	8.78	9.84	10.99
Average waterway width (m)	13.41	9.15	10	9.90	8.83	7.91
Water space area (10^3m^2)	86.84	86.88	86.87	86.89	86.92	86.91
Green space area (10^6m^2)	1.65	1.67	1.68	1.67	1.69	1.67
GR (10^6USD)	5.79	–	–	–	1.92	2.93
PP (10^6USD)	–	5.80	–	2.87	1.99	–
VS (10^6USD)	–	–	5.80	2.95	1.88	2.86
Cost of LID (10^6USD)	5.79	5.80	5.80	5.82	5.79	5.79

spatial structure. Fig. 3 1a) – 6a), 1b) – 6b) display the spatial diagram of GBI for six designs. The river network structure is developed based on the original urban canal. Therefore, the spatial organisation of the six designs is similar. The changes are mainly in the rivers that link to six outlets, but the river network outlets themselves are fixed. Fig. 3 displays the exact spatial design of green-grey-blue infrastructure. The designs below are generated for further examination against multiple temporal criteria to identify the best design.

1) Design 1 (D1): uniform distribution of GR and three separated waterway systems. The BI was planned as three independent pieces linking two outlets with the widest canals, and GR was uniformly placed on the buildings.
2) Design 2 (D2): uniform distribution of PP and two separated canal systems. The BI was constructed as two distinct pieces that link three outlets with more significant waterways, and PP was equally dispersed on primary and secondary roads.
3) Design 3 (D3): linear VS distribution with a single tree waterway system. The BI was meant to utilise a medium-width river in the north of the island to link all six outlets. The VS were planned as green corridors to link separate rivers.
4) Design 4 (D4): linear distribution of PP and VS and one tree pattern canal system. To link all distant waterways, the BI was designed with a medium-width waterway in the island's centre. The VS and PP were developed as green corridors to link separate waterways.
5) Design 5 (D5): aggregated distribution of three types of LID facilities and a looped network layout with narrow canals. The blue infrastructure system was generated as a looped pattern with several narrow rivers linking all six outlets, and multiple LID projects were placed along the waterway downstream.
6) Design 6 (D6): aggregated distribution of three types of LID facilities and a looped network with narrow waterways. The blue

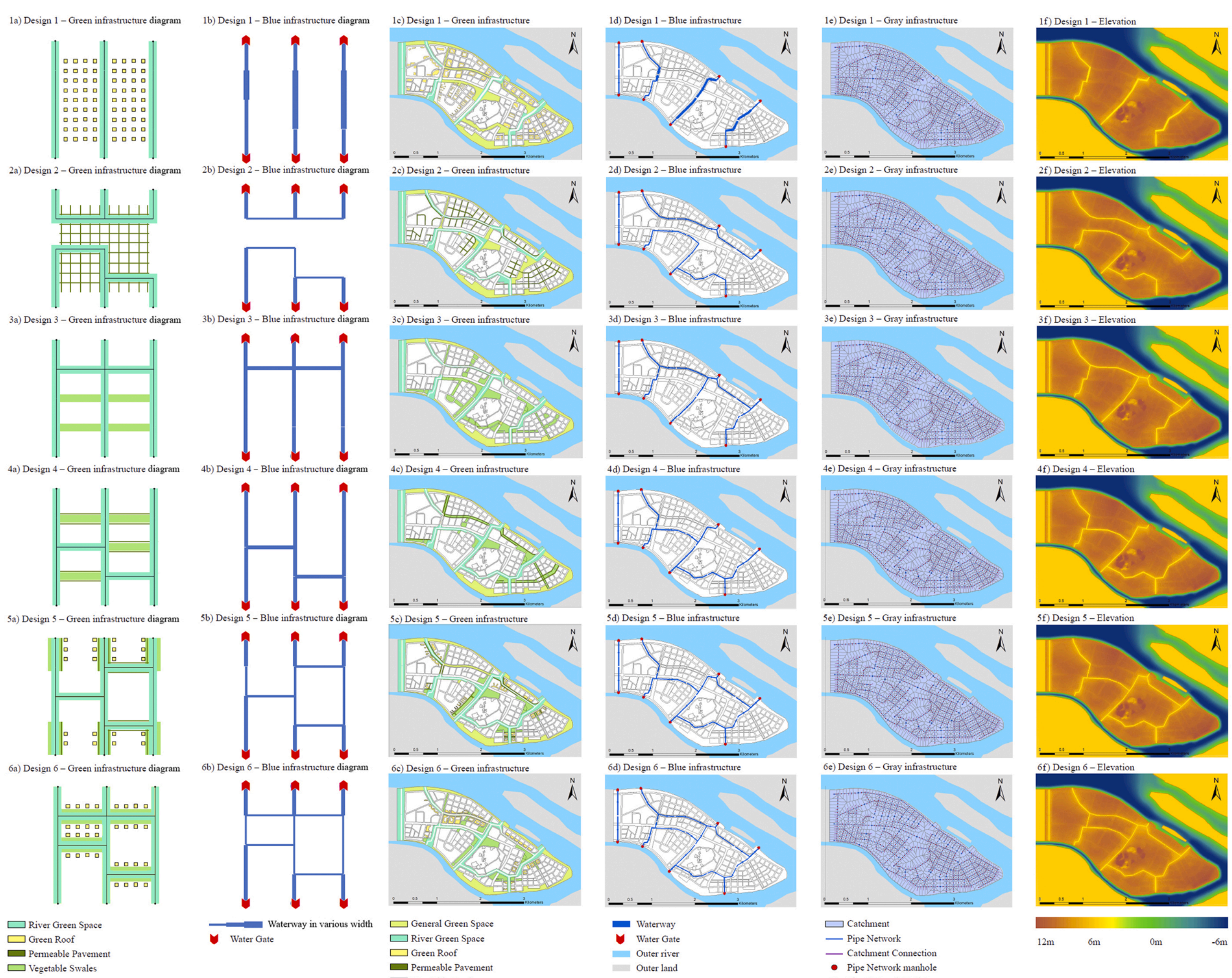

Fig. 3. Six spatial designs of green–blue-grey infrastructure for flood resilience. The spatial design diagrams of GI are shown in 1a), 2a), 3a), 4a), 5a), 6a). The spatial design diagrams of BI are shown in 1b), 2b), 3b), 4b), 5b), 6b). The deployment of LID of GI with the same cost is shown in 1c), 2c), 3c), 4c), 5c), 6c). The spatial plannings of BI waterway with the same area are shown in 1d), 2d), 3d), 4d), 5d), 6d). The pipe networks of grey infrastructure with the same design standard are shown in 1e), 2e), 3e), 4e), 5e), 6e), while the elevation designs are shown in 1f), 2f), 3f), 4f), 5f), 6f).

infrastructure system was designed as a looped pattern with multiple narrow canals to link all separated canals and various types of LID projects were created adjacent to the connected canals.

The grey infrastructure system was further developed in these six designs to fulfil the Specification for Urban Drainage Engineering Planning (GB 50318-2017), and the elevation was designed based on the GBI.

2.1.3. Definition of scenarios

The guiding standards for the flood prevention and control system in Guangzhou (2014) are developed in response to various water catastrophes. Control targets and catastrophe situations were created to analyse the flood resilience infrastructure system (Table 2). Different scenarios for the eastern section of Pazhou island were established based on disaster circumstances (rainfall intensity, river flood, and sea level rise). As stated in Eq. (1), the design rainfall intensity was estimated using the design formula from the "Central Guangzhou Rainfall Formula and Calculation Chart." The water level at the Huangpu Gauging Station was utilised to build the primary tidal curve. The design flood level in the outer river was determined in line with Guangzhou's River system planning. Based on sea level measurements in the Pearl River Delta over the past three decades and an increasing mean rate of 2.5 mm/a, the river level is projected to rise 200 mm by 2100. (Dong et al., 2012). Peak rainfall was scheduled to coincide with the tidal curve to maximise the effect of the catastrophe situations and recreate the worst-case scenario. The Chicago storm profile is employed in this research to generate rainfall hydrographs. The equation below computed the rainfall intensity of 50-year return periods with a 2-hour rainfall duration.

$$Q = \frac{21.740}{(t + 6.274)^{0.598}} \quad (1)$$

where Q is storm rainfall intensity (mm/min); and t is the rainfall duration, min;

2.1.4. Control objectives

Considering a city as a socio-technical-ecological system (Berkes, Folke, & Colding, 2000), we think that a green-grey-blue infrastructure system may play an essential role in balancing the impacts of natural hazards with the needs of urban life. Most study on the dynamic process of urban flood resilience focuses on three categories: absorbing excessive rainfall, preserving operational function, and lowering and recovering from the damage (Bertilsson, et al., 2019).

Each category has its own set of performance measurements. The ability to absorb surplus rainfall is typically quantified in runoff volume reduction and green space storage capacity. For example, Shishegar, Duchesne, and Pelletier (2018) employed runoff reduction to improve stormwater management measures, while Khadka et al. (2019) demonstrated how storage capacity supports flood resilience. Also recognised as indicators of hydrological functions are water discharge and river storage depth. The ratio of the water amount from the rainfall discharge to the area of the regional river is known as the river storage depth.

The fact that performance assessment of flood resilience predominantly depends on the green-grey-blue infrastructure system poses various problems. Integrative assessments are necessary from the whole city's viewpoint, considering both land-based and hydrological variables. This research incorporated land use data into a flood resilience assessment technique, highlighting the necessity to analyse the city's influence. To estimate the effect of rainfall and river floods, the overflow volume from the infrastructure system onto roads and the submerged area in development areas were selected.

Runoff reduction is estimated from the SWMM model embedded in Mike Urban. The calculation formulas are shown in Table 3; they were utilised in the raster calculator in GIS to compute additional indicators.

Table 2
Three scenarios based on the design rainfall, design river flood, and predicted sea level rise.

Scenario	Rainfall	River flood Level	Sea level Rise
Scenario1 (S1)	50-year 2 h design rainfall	Normal river level	Sea level in 2020
Scenario2 (S2)	50-year 2 h design rainfall	5-year flood	Sea level in 2020
Scenario3 (S3)	50-year 2 h design rainfall	5-year flood	Sea level in 2100

2.2. Coupled hydrodynamic model simulation

Establishing a quantitative cause-and-effect relationship via mechanistic mathematical modelling is essential to support successful decision-making on urban flood resilience. The performance of the green-grey-blue infrastructure system was simulated using a connected model that included rainfall-runoff, an urban overland model, a drainage system model, and a river system model, respectively. (Formulas see Supplementary material 1.2).

2.2.1. Construction of the coupled model

MIKE 11, a one-dimensional river model, requires BI data, such as waterway network data and hydrological boundary data (Fig. 3 1d) – 6d)). Several water gates were installed in the outlets to keep the gates open until the water level within exceeded the tidal level. The BI's hydrological boundary condition was determined using various scenarios (Details see Supplementary material 1.1).

MIKE Urban, a one-dimensional drainage network and rainfall-runoff model, requires grey infrastructure data, such as pipe network data, catchment data (Fig. 3 1e) – 6e)), and rainfall data (Details see Supplementary material 1.1).

The MIKE 21, a two-dimensional overflow model, requires surface elevation and resistance data to simulate overflow water on GI and other urban lands. The urban surface elevation was generated at a spatial resolution of 4 m × 4 m utilising design elevation and sunken green space variation (Fig. 3 1c) – 6c), 1f) – 6f)). The simulation time step was set to one second, and the total duration was set to seven hours, including a one-hour warm-up period. The surface resistance was determined as Manning's n to depend on land use data (see Supplementary material 1.3).

MIKE Flood, as an integrated platform combining MIKE 11, MIKE 21, and MIKE Urban, offers a variety of linkages to simulate the interaction among diverse urban drainage subsystems dynamically. Lateral connections simulate rivers overflowing to river green spaces. River-urban linkages represent the outflow of water from drainage pipes to waterways, while standard links model the outflow of water from waterways to outer rivers. Urban linkages simulate the overflow of water from drainage pipes onto urban surfaces.

Table 3
Calculation method of the indicators.

Indicators	Formula
water storage in BI	$V(b) = \sum_i \sum_j d_{ij} * Sifl_{ij} = 1$
water storage in GI	$V(g) = \sum_i \sum_j d_{ij} * Sifl_{ij} = 2$
overflow volume in road	$V(r) = \sum_i \sum_j d_{ij} * Sifl_{ij} = 3$
submerge area in development land	$A(d) = \sum_i \sum_j Sifl_{ij} = 4 and d_{ij} > 0.01$

Where $D = [d_{ij}]$ (m) is a water depth matrix, I and j represent column and row number of raster; $L = [l_{ij}]$, $l \in \{1,2,3,4\}$ is a land matrix used to represent the various types of land, including water space: 1, green space: 2, road: 3, development land: 4; and S (m^2) is the area of each raster.

2.2.2. Model accuracy

Model accuracy is the foundation of our work; it can be attained by calibration and verification. Because the urban design scenario in the model is not a practical scenario, it is assumed that its model parameters can be obtained from adjacent areas with similar degrees of urban development. Two calibration areas around the study area were selected, and model calibration of Mike flood and SWMM were done by Lei et al. (2021) and Zhang, Lin, Huirong, and Wang (2019). The main parameter setup was based on this research and verified to ensure reliability. Model validation was undertaken for the whole integrated model in a nearby area, with information including water discharge records, water depth, and a historical rainfall on May 22, 2020, obtained from Zengcheng District Water Bureau. The Nash–Sutcliffe efficiency (NSE) and relative error (RE) are often used to validate urban drainage system models. Results of the validation indicate that the RE is 17% and NSE is 0.95, which proves that this model can serve as a computational platform for further study. (Details see Supplementary material 2).

2.3. Temporal MCDM

The temporal MCDM is an extension of the traditional MCDM. In contrast to other MCDMs, TOPSIS makes full use of attribute information, provides a cardinal ranking of choices, has high resilience, and is easy to compute and utilise for decision analysis (Deng, Yeh, & Robert, 2000). As a result, we expand TOPSIS to temporal scales to account for dynamic indicators. The input matrix of the temporal TOPSIS is a three-dimensional matrix X, including the information about five temporal indicators with six designs during simulation time. The optimum temporal TOPSIS alternative should be the shortest distance from the positive-ideal solution and the longest distance from the negative-ideal solution, depending on whether the criterion favours benefit or cost. The benefit set covers runoff reduction, water storage in BI, and water storage in GI, whereas the cost set contains overflow volume in roads and submerged areas in development land. The steps of the temporal TOPSIS are presented in Supplementary material 3.1. (Betania, Leonardo, & João, 2023; Jarosław, Aleksandra, Ewa, & Wojciech, 2022).

Another aspect of the temporal TOPSIS method and its expansion is that it incorporates relative weights that reflect each criterion's importance in each timestep (Olson, 2004). The objective entropy weighting approach determines criteria significance weights based on data contained in input matrices for each timestep. This is a common weighing approach for assessing value dispersion in decision-making. The larger the degree of dispersion, the greater the degree of differentiation and the larger the amount of information that can be extracted. Meanwhile, the index should be given more weight, and vice versa (Zhu, Tian & Yan, 2020). The entropy weighting method is described in Supplementary material 3.2. (Farhad & Reza, 2010).

3. Results

3.1. Results of the TOPSIS assessment of different designs

The flood resilience designs were rated using the temporal TOPSIS. Fig. 4 1a) and 1b) illustrate that D5 proves to be the best solution during the rainstorm, and D2 performs better after the rainfall. It may be concluded that adequate BI connections and GI distribution can enhance the flood performance of the infrastructure system. Improving BI connection and placing GI downstream may assist in developing a robust

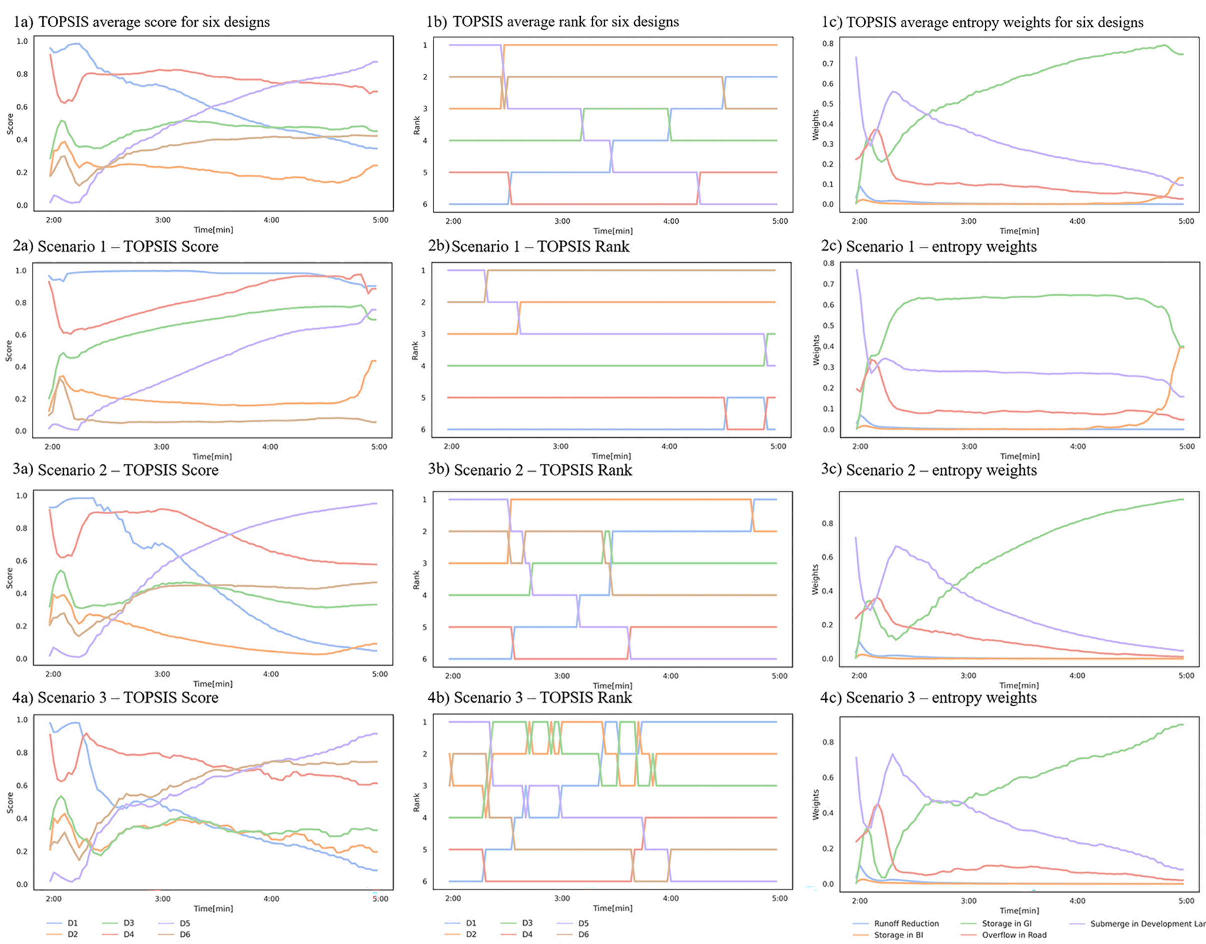

Fig. 4. The average result and the results for three scenarios of Temporal TOPSIS for six designs.

system during peak rainfall while expanding the canal width with ample river green space can help strengthen flood resilience after the storm. However, if the waterway is so broad that it affects the river canal connectivity and the area of river green space, the flood performance will be undermined. Fig. 4 1c) demonstrates the variance in the weights of several indicators. Overflow on roads and submerged areas in development land have a higher weight during peak rainfall. However, following the rainfall, the storage of BI increased as an essential factor.

Fig. 4 2a) – 4c) presents the complete finding of the temporal TOPSIS for three scenarios. The scores of various designs vary substantially in the three scenarios. D1 and D5, D2 and D3 exhibit different tendencies in S2 and S3, whereas D3 and D4, D5, and D6 show similar trends in S3. This may be explained by the fact that while confronting an intense water crisis, the spatial structure of the BGI can considerably impact the trend of the score, and the same spatial structure tends to behave similarly. Regarding the entropy weights, various designs have the same temporal trends but differ slightly at the end.

3.2. Reducing runoff

Fig. 5 displays the runoff volumes for various designs. The LID facilities minimise rainfall-runoff between 105 mm and 111 mm, although total rainfall is 145 mm, according to model data. These data show that the LID cannot perform correctly under such a severe downpour during the runoff phase. Compared to the BI design, the LID configuration's effectiveness is marginally diminished by external hydrological circumstances such as river floods and sea level rise. Due to the urbanisation of the research region, this is a relatively moderate runoff reduction. Even though all levels of LID implementation reduce runoff, when compared to D1, D2, and D3, the highest relative runoff reduction occurs in D3 (VS) with the same cost of LID deployment, and the performance of the GR and PP is comparably weak. Furthermore, owing to the relatively moderate performance, it is not easy to detect the advantage of D4, D5 and D6. The multiplicity of LID solutions allows for forming a broad spatial structure that can hold water when water levels surpass those converging in BI, as detailed below.

3.3. Water storage

3.3.1. Water storage in blue infrastructure

Fig. 6 1a) – 3a) compares six BI spatial designs in three scenarios for water storage. The demand for BI to store rainwater is growing as the outside water level increases. S3 exhibits a more pronounced volume peak and a 20-minute delay in peak time relative to S1, indicating that the extreme hydrological boundary condition demands the infrastructure to store water for a longer duration rather than simply draining water away from the metropolitan system.

Specific spatial structures and essential linkages of the common waterway emerge when comparing the simulation results of various designs in each scenario with the same area of water space. When comparing D1 and D2, the storage capacity could be enhanced by connecting two catchments with a broader urban canal, and the joints would be better located downstream of the river. When comparing D3 to D5 and D6, the looping network has a larger water storage capacity than the tree structure. In this specific research location, a high connectivity network (two loops) does not efficiently raise water storage capacity over a lower one. However, increased storage capacity through a multi-loop system cannot be ruled out. The findings show that a crucial connection may boost capacity in the spatial design of BI while also being directed by an appropriate typical structure. In contrast to S2 and S3, water storage is approaching the BI capacity limit. GI is required to increase water storage capacity temporarily.

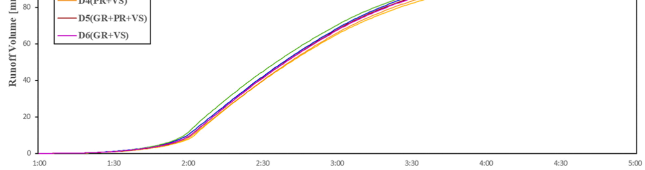

Fig. 5. The runoff volume simulation results.

3.3.2. Water storage in green infrastructure

Fig. 6 1b) – 3b) illustrates the variance in GI water storage when external hydrological conditions alter. The quantity of water storage increases slightly from S1 to S2, whereas it climbs dramatically from S2 to S3, from roughly 26 10^3 m^3 to over 100 10^3 m^3. The trend suggests that GI's water storage capacity is an essential complement to BI and a significant component of infrastructure system flood resilience in the case of potential excessive rains.

The storage capacity limit of BI and the extent of green space adjacent to the canal influence the water storage capacity of GI. Comparing D1 with other designs in S1 shows that GI might supply extra water storage space when BI's capacity is achieved. Due to a scarcity of riverbank green space aligned to the canal, the water storage capacity of GI progressively approaches its maximum limit of 60 10^3 m^3 in S2 and S3. The water storage of green–blue-grey infrastructure can be determined precisely by combining the water storage capacity of GBI, which is 440 10^3 m^3 based on external hydrological conditions. However, the water storage capacity is not proportionate to the river's length. When comparing D5 and D6, the longest river cannot offer adequate green space for retaining extra water. When comparing D2 and D4, appropriate canal spatial arrangement may maximise the utilisation of green space and raise water storage capacity.

The distribution of water storage in GI (Fig. 7) shows that the bulk of the storage space is situated downstream of the canal, especially around the waterway's confluence and discharge to the outer river. In addition, geographical distribution has a considerable influence on water storage. When comparing D1 and D2, the essential link between different catchments near the outlets can balance the runoff volume between various catchments and make full use of the green space near the outlets, and when comparing D3 and D4, it can make full use of the green space near the outlets. On the other hand, the connections distant from the outlet do not contribute to flood resilience.

3.4. Urban impact

3.4.1. Overflow volume

Fig. 8 compares the water overflow volume of six alternative designs under various scenarios, demonstrating that the amount of overflow is mainly influenced by the length of the canal and has little to do with external hydrological circumstances. Because the green–blue-grey infrastructure cannot store excess runoff, the most significant difference between S1 and S3 is around 2:30, which increases dramatically in S3 and decreases gradually in S1 and S2. Another distinction between S1 and S3 is the volume peak, which increases slightly. The volume of overflow is proportional to the waterway's length. With the same water area, D1 has a 19 10^3 m^3 overflow volume with a 6476.68 m canal, D5 has an 8 10^3 m^3 overflow volume with a 9844.64 m waterway, and D3 and D4 have a virtually similar overflow volume with a 6476.68 m waterway. However, D6 is an exception, implying that certain waterways may not function during heavy rains, endangering the infrastructure system's functionality.

3.4.2. Submerged area

Fig. 9 indicates the breadth and duration of submerged development land in the study area of six designs. External hydrological conditions and the spatial organisation of the city region primarily govern the

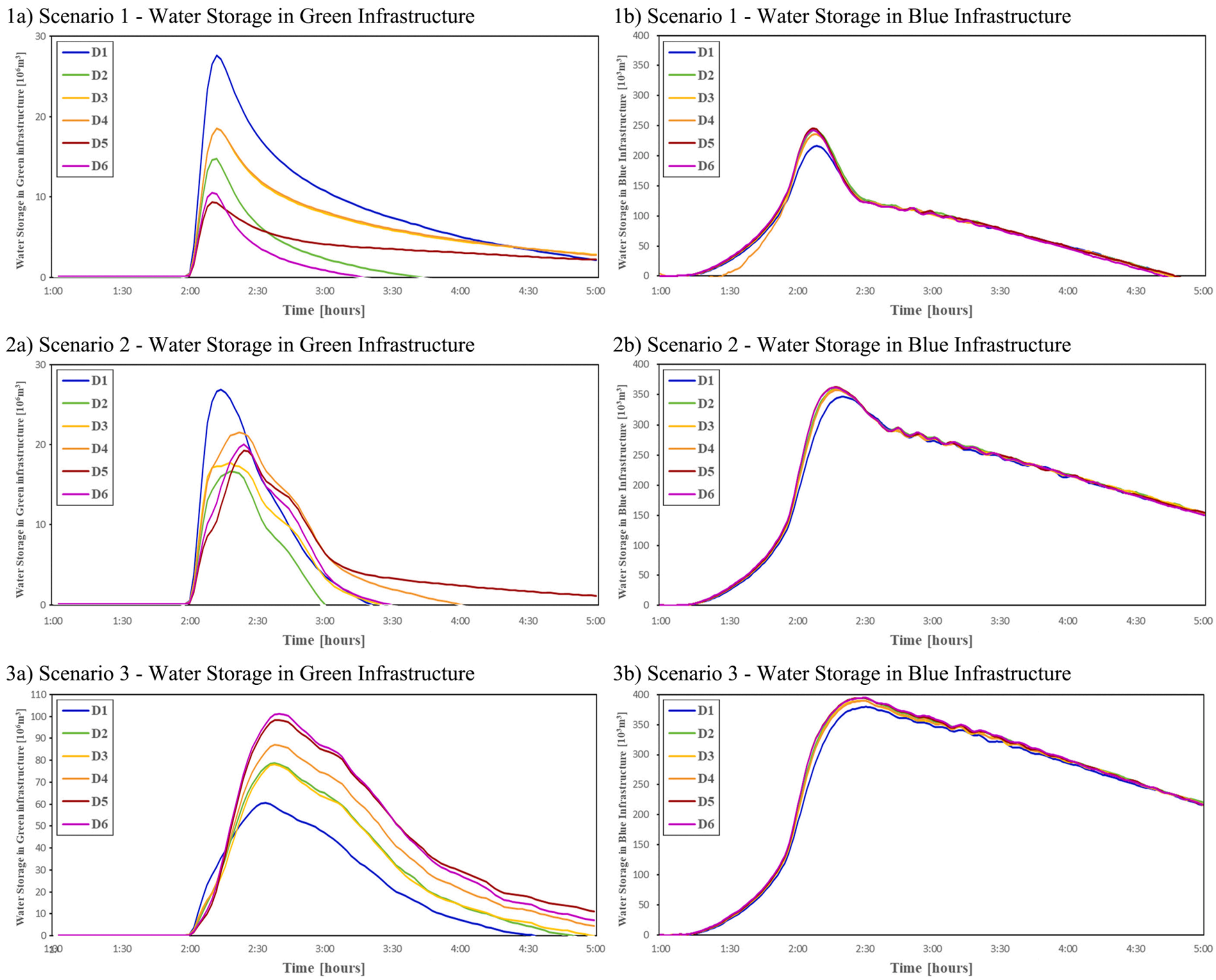

Fig. 6. The simulation results of GI's and BI's water storage of six designs under three scenarios.

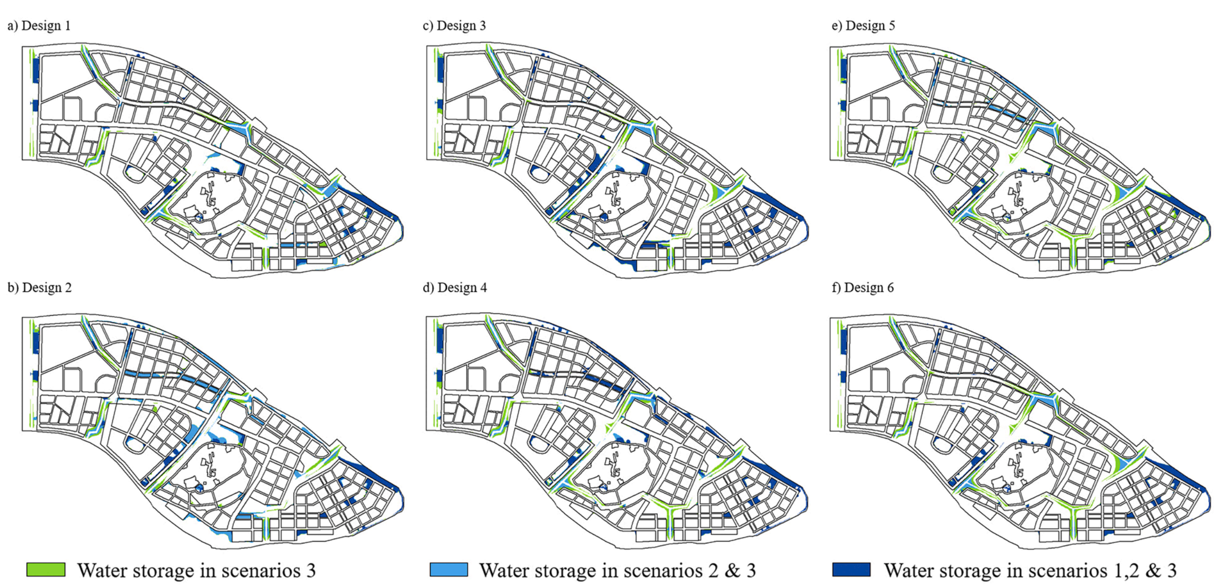

Fig. 7. The simulation results of the distribution of BI's water storage of six designs under three scenarios.

extent and duration of urban floods. In D3, D5 and D6 of S1, compared to S2 and S3, the submerged area expanded considerably, while the duration of the submerged area extended only modestly.

Fig. 9 highlights that the design performance of flood resilience has little to do with design indicators like total area of water or green space, waterway length or width, or LID deployment but rather depends on the spatial structure of green–blue-grey infrastructure, including some critical waterway connections and green space distribution. It is simple

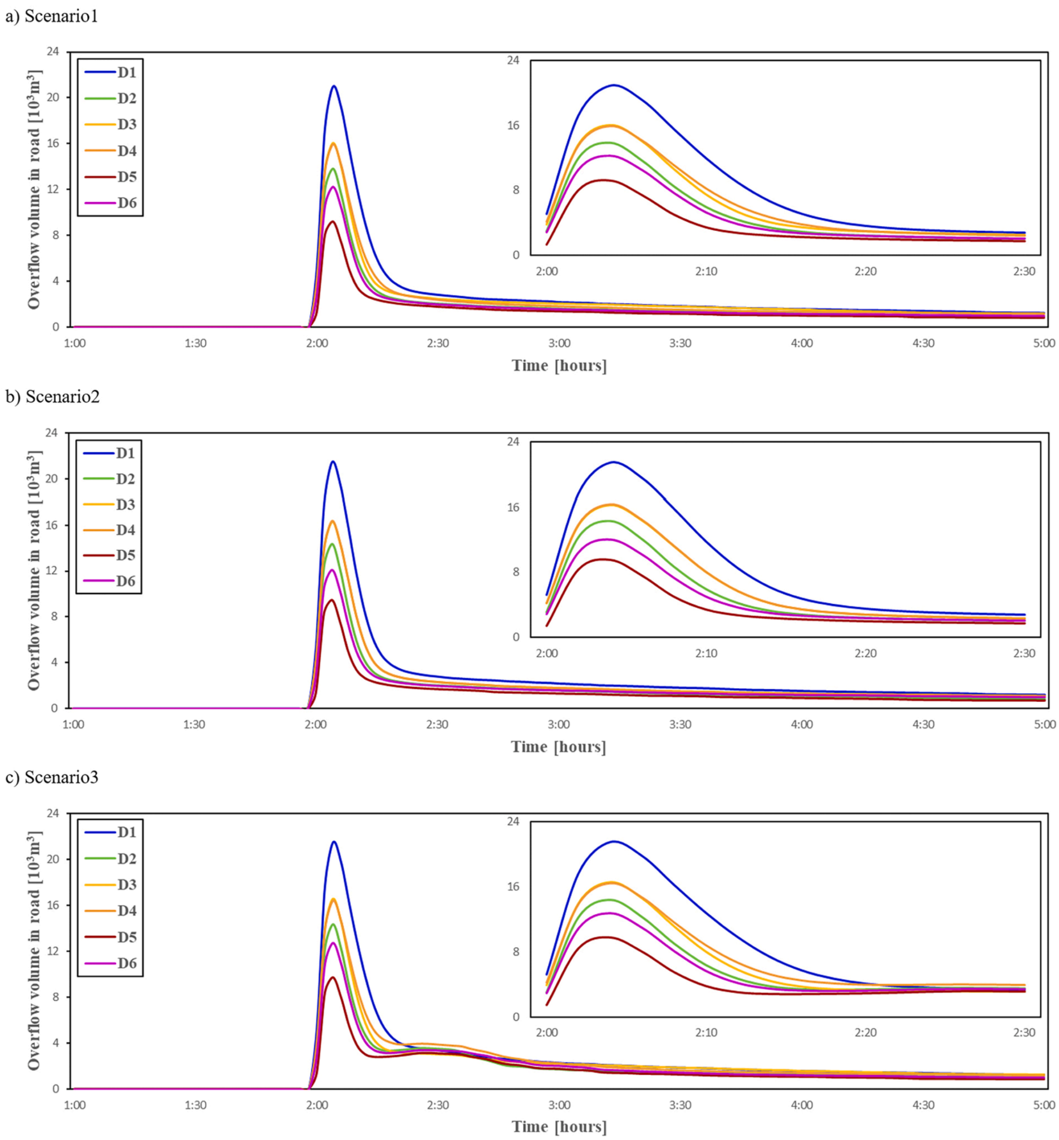

Fig. 8. The simulation results of the water overflow volume of six designs under three scenarios.

to divide six designs into three groups and discover the necessary canal and green space by searching for comparable features in each design in the same group.

The spatial organisation of blue-green-grey infrastructure determines the degree of urban flooding (Fig. 10). The increase in the canal water level resulted in the submergence of roads and lands along the drainage system, which had its outlets at the downstream end of the waterway. However, in the southern half of the research area, there is a historic town whose elevation cannot be adjusted. Compared to D3 and D4, it can be established that conserving and widening the original river encircling the hamlet is a reasonable alternative to decrease the flooding of historic urban buildings and roadways. Furthermore, in the case of a looping network, the duplicate canal would limit water storage capacity and exacerbate urban inundation in the same watershed region.

4. Discussion

This study aimed to determine the optimal resilience solution by evaluating the flood performance of the green-grey-blue infrastructure system from various spatial designs. This study demonstrates the importance of taking a holistic view of resilience performance in the green-grey-blue infrastructure system; providing a temporal MCDM method for achieving the optimal spatial design of the urban environment, as well as some spatial recommendations for policymakers and urban designers to improve resilience.

4.1. A scenario-based assessment framework as a holistic perspective

This research enables decision-makers to find the ideal solution by balancing viewpoints from various disciplines. Some academics consider one unique system in flood control, such as grey infrastructure or LID (Pugliese, Gerundo, Paola, Caroppi, & Giugni, 2022). Other studies underline the relevance of the overall infrastructure system but only examine one scenario (Haghighatafshar et al., 2018). In this study, we investigate six designs with three scenarios to offer a comprehensive view to the decision-maker and employ a green-grey-blue system to lay open the performance of flood resilience. According to this study, LID in GI is less effective in controlling runoff during extremely heavy rainfalls. However, restructuring the green space is a realistic, valid option to increase redundancy for exceeding precipitation. These conclusions are also validated by earlier investigations (Lu & Sun, 2021; Liu, Chen, & Peng, 2014).

The temporal TOPSIS is another expansion of our framework. Usually, MCDM approaches rank the alternatives without considering their

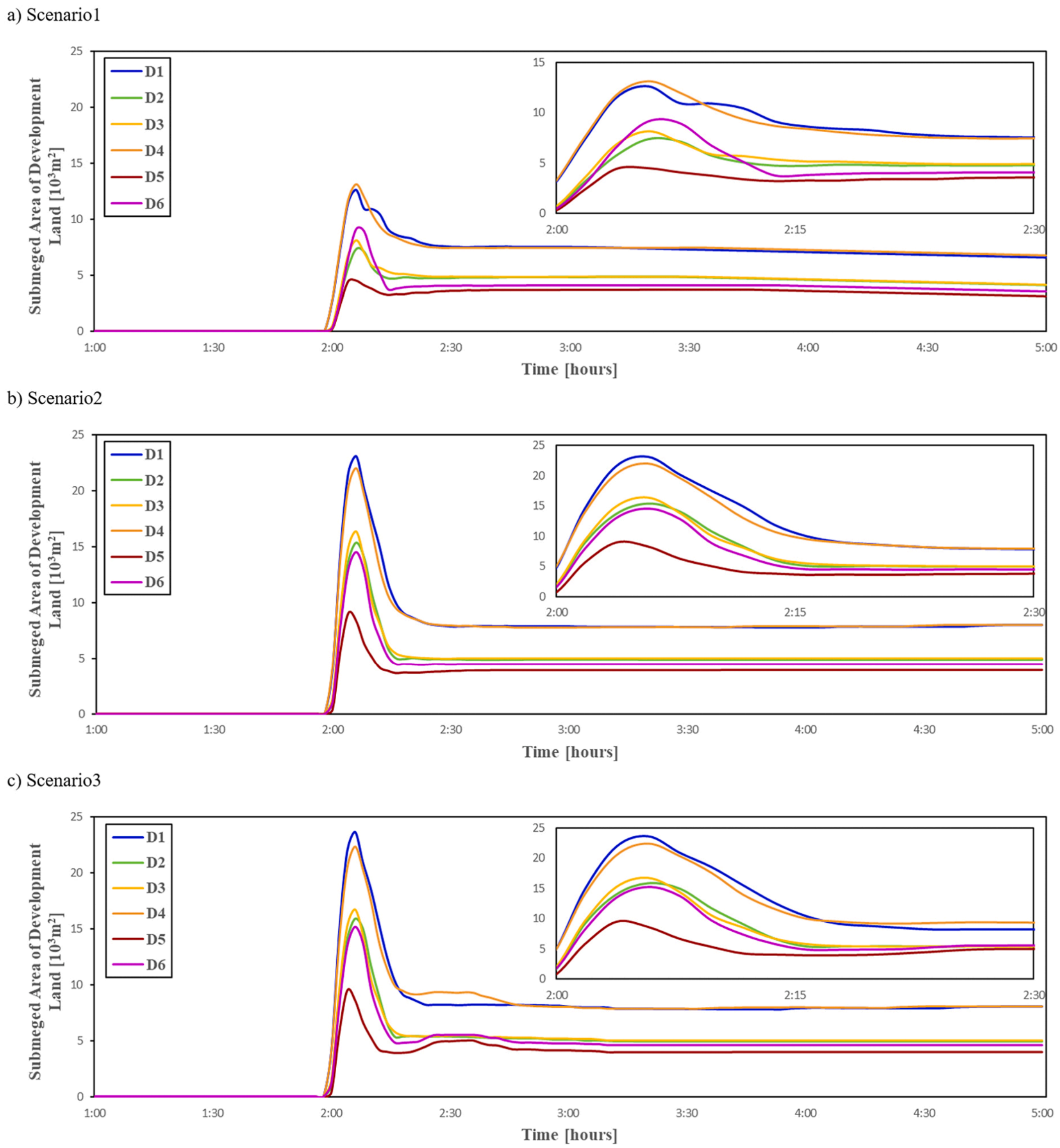

Fig. 9. The simulation results of the submerged area of six designs under three scenarios.

evolution over time, which may provide critical information for the decision-maker (Betania, Leonardo, & João, 2023). Our research demonstrates the dynamic process of alternative ranking and entropy weights during and after heavy rainfall, suggesting submerged areas in development land and overflow volume in the road are essential during the rainfall, and water storage in GI appears essential after the rainfall. This phenomenon was also found in past studies (Matthews, 2016), demonstrating some degree of temporal TOPSIS accuracy. However, as this is a novel extension to TOPSIS, it needs to be employed in more studies in the future to show its correctness.

In a word, green-grey-blue infrastructure design must employ a systematic approach to accomplish integrated management and sustainability of the urban water environment. This approach may be adapted to different locations to undertake comparative research.

4.2. Improving the resilience of green-grey-blue infrastructure by spatial design

Some studies highlight the hydrological and configuration parameters of BI to determine the ideal option, but few works have focused on the spatial structure of BI (Alves, Vojinovic, Kapelan, Sanchez, & Gersonius, 2020). Our research has explored six distinct BI spatial designs with the same area of water space and green space and the same cost of LID to demonstrate that resilience can be enhanced by reorganising the spatial structure of BI. The flood performances demonstrate that connectivity is the major component in boosting resilience, and the looping network demonstrates greater resilience than the tree network and separate network. Other large-scale investigations have revealed comparable effects (Dong, Yu, Farahmand, & Mostafavi, 2019). Furthermore, the simulation findings revealed that connectivity had a limit and that certain connections, like the downstream junction, performed better than others. Other case studies support these fascinating results (Haghighatafshar et al., 2018).

The co-benefits of several infrastructure systems might be a bonus for flood resilience (Alves, Gersonius, Kapelan, Vojinovic, & Sanchez, 2019). According to several studies, the collaborative design of a grey-green infrastructure system, including placing utility holes in sunken green space or redesigning green corridors with aligned drainage pipes, can establish a robust system to cope with water catastrophes (Lu & Sun, 2021). Our study illustrates that resilience can be enhanced by replacing river green space.

Our findings also show that specific LID configurations are

Fig. 10. The simulation results of the distribution of submerged area of six designs under three scenarios.

ineffective in enhancing flood resilience. Other studies further demonstrate that when rainfall intensity increases, the runoff-control efficacy of LID systems is reduced (Jingming et al., 2019). The distribution of river green space is vital. The urban canal downstream serves as an excellent redundant region for retaining excess precipitation. Additionally, the appropriate distribution might constrict the urban inundation near waterways and reduce the submerged area. These findings should be discussed in collaboration between urban designers and hydrological engineers and considered in the early stages of urban planning.

4.3. Limitations of the study

This research did not take water quality into consideration, even though it is a crucial component in determining flood risk and frequently causes economic and lives losses following severe rain and river floods (Leng, Xu, Jia, & Jia, 2022; Pugliese, Gerundo, Paola, Caroppi, & Giugni, 2022). However, using the hydrodynamic model as the foundation for the hydrology model allows us to add water quality into future investigations. Water depth and velocity are significant for accounting for water catastrophe losses (Lazzarin, Viero, Molinari, Ballio, & Defina, 2022). Due to outstanding spatial planning and ideal infrastructure maintenance, water depth is minimised in the early phases of urban design. Future research will consider this issue to replicate and analyse a more realistic urban environment.

5. Conclusion

This study developed an integrated scenario-based assessment framework to assess the flood performance of various spatial solutions of infrastructure systems and rank the solutions based on dynamic performance. Our study reveals the relationship between the spatial structure of the green-grey-blue infrastructure system and flood performance in spatiotemporal scales. It delivers beneficial conclusions for decision-makers and urban planners based on a case study of GBA, China. According to the research, different blue-green-grey infrastructure designs with the same amount of water and green space and the same cost of LID demonstrate vastly varying flood resilience performance, notably in water storage capacity and the size and duration of submerged land. The spatial distribution of LID facilities did not play a significant role in the runoff reduction during heavy rain, while BI supplements GI to retain more water during and after a downpour. Extreme rainfall and externally harsh hydrological conditions can be handled partly by storing water in BI and connecting waterways of critical links. It is possible to determine the crucial spatial structure by considering dynamic processes using temporal TOPSIS. Furthermore, the temporal TOPSIS can also reveal the varying importance of each indicator per case. Based on the expected scenarios and site characteristics, the desired spatial design for flood resistance generated from the suggested performance evaluation methodology can be customised to another location.

Declaration of Competing Interest

This work was financially supported by the National Natural Science Foundation of China (grant numbers: 51761135025, 51778233), the Dutch Research Council (grant number: ALWSD 2016.013), and Guangdong Science and Technology Department (grant numbers: 2020B1010010002). The authors declare that they have no known competing financial interests or personal relationships that could have appeared to influence the work reported in this paper.

Data availability

Data will be made available on request.

Appendix A. Supplementary data

Supplementary data to this article can be found online at https://doi.org/10.1016/j.landurbplan.2023.104804.

References

Alves, A., Gersonius, B., Kapelan, Z., Vojinovic, Z., & Sanchez, A. (2019). Assessing the co-benefits of green-blue-grey infrastructure for sustainable urban flood risk management. *Journal of Environmental Management, 239*, 244–254. https://doi.org/10.1016/j.jenvman.2019.03.036

Alves, A., Vojinovic, Z., Kapelan, Z., Sanchez, A., & Gersonius, B. (2020). Exploring trade-offs among the multiple benefits of green-blue-grey infrastructure for urban flood mitigation. *Science of The Total Environment, 703*, Article 134980. https://doi.org/10.1016/j.scitotenv.2019.134980

Berkes, F., Folke, C., & Colding, J. (Eds.). (2000). *Linking social and ecological systems: Management practices and social mechanisms for building resilience*. Cambridge University Press.

Bertilsson, L., Wiklund, K., de Moura Tebaldi, I., Rezende, O. M., Veról, A. P., & Miguez, M. G. (2019). Urban flood resilience – A multi-criteria index to integrate flood resilience into urban planning. *Journal of Hydrology, 573*, 970–982. https://doi.org/10.1016/j.jhydrol.2018.06.052

Betania, S. C., Leonardo, T. D., & João, M. T. (2023). Exploiting temporal features in multicriteria decision analysis by means of a tensorial formulation of the TOPSIS method. *Computers & Industrial Engineering, 175*.

Campello, B. S., Duarte, L. T., & Romanoa, J. M. (2022). Exploiting temporal features in multicriteria decision analysis by means of a tensorial formulation of the TOPSIS method. *Computers & Industrial Engineering.* , Article 108915. https://doi.org/10.1016/j.cie.2022.108915

Casal-Campos, A., Fu, G., Butler, D., & Moore, A. (2015). An integrated environmental assessment of green and gray infrastructure strategies for robust decision making. *Environmental science & technology, 49*(14), 8307–8314. https://doi.org/10.1021/es506144f

CECS (2021). Technical guidelines for selection method of sponge city low impact development facilities, China Association for Engineering Construction (author: China Association for Engineering Construction; standard number: T/CECS 866-2021) Standardization.

Chen, W., Wang, W., Huang, G., Wang, Z., Lai, C., & Yang, Z. (2021). The capacity of grey infrastructure in urban flood management: A comprehensive analysis of grey infrastructure and the green-grey approach. *International Journal of Disaster Risk Reduction, 54*, Article 102045. https://doi.org/10.1016/j.ijdrr.2021.102045

Chen, Y., Li, J., & Chen, A. (2021). Does high risk mean high loss: Evidence from flood disaster in southern China. *Science of the Total Environment, 785*, Article 147127. https://doi.org/10.1016/j.scitotenv.2021.147127

Deng, H., Yeh, C.-H., & Robert, J. (2000). Inter-company comparison using modified TOPSIS with objective weights. *Computers & Operations Research, 27*(10), 963–973. https://doi.org/10.1016/S0305-0548(99)00069-6

Dong, H., Huang, C., Chen, W., Zhang, H., Zhi, B., & Zhao, X. (2012). The controlling factors of environment geology in the Pearl River Delta Economic Zone and an analysis of existing problems. Retrieved from *Geology in China, 39*(2), 539–549 http://geochina.cgs.gov.cn/geochinaen/article/pdf/20120225.

Dong, S., Yu, T., Farahmand, H., & Mostafavi, A. (2019). Bayesian modeling of flood control networks for failure cascade characterization and vulnerability assessment. *Computer-Aided Civil and Infrastructure Engineering, 35*(7), 668–684.

Driessen, P. P., Hegger, D. L., Kundzewicz, Z. W., Van Rijswick, H. F., Crabbé, A., Larrue, C., … Wiering, M. (2018). Governance strategies for improving flood resilience in the face of climate change. *Water, 10*(11), 1595. https://doi.org/10.3390/w10111595

EM-DAT. (2019). *Human cost of disasters: an overview of the last 20 years (2000-2019)*. Retrieved from CRED Emergency Events Database.: https://www.emdat.be/.

Farhad, H. L., & Reza, F. (2010). Imprecise Shannon's entropy and multi attribute decision making. *Entropy*, 53–62.

Fletcher, T. D., Shuster, W., Hunt, W. F., Ashley, R., Butler, D., Arthur, S., … Viklander, M. (2015). SUDS, LID, BMPs, WSUD and more – The evolution and application of terminology surrounding urban drainage. *Urban Water Journal, 12*(7), 525–542. https://doi.org/10.1080/1573062X.2014.916314

Girona's, J., Roesner, L. A., Rossman, L. A., & Davis, J. (2010). A new applications manual for the Storm Water Management Model (SWMM). *Environmental Modelling & Software, 25*(6), 813–814. https://doi.org/10.1016/j.envsoft.2009.11.009

Government, GuangZhou (2017). Guangzhou Sponge City Planning and Design Guidelines. Standardization.

Haghighatafshar, S., Nordlöf, B., Roldin, M., Gustafsson, L. G., la Cour Jansen, J., & Jönsson, K. (2018). Efficiency of blue-green stormwater retrofits for flood mitigation – Conclusions drawn from a case study in Malmö, Sweden. *Journal of Environmental Management, 207*, 60–69. https://doi.org/10.1016/j.jenvman.2017.11.018

Huang, I. B., Keisler, J., & Linkov, I. (2011). Multi-criteria decision analysis in environmental sciences: Ten years of applications and trends. *Science of The Total Environment, 409*(19), 3578–3594. https://doi.org/10.1016/j.scitotenv.2011.06.022

Jarosław, W., Aleksandra, B., Ewa, Z., & Wojciech, S. (2022). Temporal VIKOR - A New MCDA Method Supporting Sustainability Assessment.

Javari, M., Saghaei, M., & Fadaei Jazi, F. (2021). Analyzing the resilience of study: Malayer city). *Sustainable Environment, 7*(1), Article 1889083. https://doi.org/10.1080/27658511.2021.1889083

Jingming, H., Donglai, L., Xiaojun, W., Kaihua, G., Yu, T., & Yue, M. (2019). Effects of initial conditions of LID measures on runoff control at residential community scale. *Advances in Water Science, 30*(1), 45–55. https://doi.org/10.14042/j.cnki.32.1309.2019.01.005

Johannessen, A., & Wamsler, C. (2017). What does resilience mean for urban water services? *Ecology and Society, 22*(1).

Joyce, J., Chang, N.-B., Harji, R., & Ruppert, T. (2018). Coupling infrastructure resilience and flood risk assessment via copulas analyses for a coastal green-grey-blue drainage system under extreme weather events. *Environmental Modelling & Software, 100*, 82–103. https://doi.org/10.1016/j.envsoft.2017.11.008

Karamouz, M., Taheri, M., Khalili, P., & Chen, X. (2019). Building infrastructure resilience in coastal flood risk management. *Journal of Water Resources Planning and Management, 145*(4), 04019004. https://doi.org/10.1061/(ASCE)WR.1943-5452.0001043

Khadka, A., Kokkonen, T., Niemi, T. J., Lähde, E., Sillanpää, N., & Koivusalo, H. (2019). Towards natural water cycle in urban areas: Modelling stormwater management designs. *Urban Water Journal, 17*(7), 587–597. https://doi.org/10.1080/1573062X.2019.1700285

Kuwae, T., & Crooks, S. (2021). Linking climate change mitigation and adaptation through coastal green–gray infrastructure: A perspective. *Coastal Engineering Journal, 63*(3), 188–199.

Lazzarin, T., Viero, P. D., Molinari, D., Ballio, F., & Defina, A. (2022). Flood damage functions based on a single physics- and data-based impact parameter that jointly accounts for water depth and velocity. *Journal of Hydrology, 607*, Article 127485. https://doi.org/10.1016/j.jhydrol.2022.127485

Lei, X., Lai, C., Wang, Z., Zeng, Z., Lin, G., & Zhao, J. (2021). Influence of LID adaptation on urban flooding and non-point source pollution. *Water Resources Protection, 37* (05), 131–139. https://doi.org/10.3880/j.issn.10046933.2021.05.020

Leng, L. H., Chen, A. S., Zhu, D. Z., Xu, T., & Yu, S. (2021). Multi-objective optimization for green-grey infrastructures in response to external uncertainties. *Science of The Total Environment, 775*, Article 145831. https://doi.org/10.1016/j.scitotenv.2021.145831

Leng, L., Mao, X., Jia, H., Xu, T., Chen, A. S., Yin, D., & Fu, G. (2020). Performance assessment of coupled green-grey-blue systems for Sponge City construction. *Science of the Total Environment, 728*, Article 138608. https://doi.org/10.1016/j.scitotenv.2020.138608

Leng, L., Xu, C., Jia, H., & Jia, Q. (2022). Incorporating receiving waters responses into the framework of spatial optimization of LID-BMPs in plain river network region. *Water Research, 224*, Article 119036. https://doi.org/10.1016/j.watres.2022.119036

Li, W., Yi, P., & Zhang, D. (2018). Sustainability evaluation of cities in Northeastern China using dynamic TOPSIS-entropy methods. *Sustainability, 10*(12), 4542. https://doi.org/10.3390/su10124542

Liu, W., Chen, W., & Peng, C. (2014). Assessing the effectiveness of green infrastructures on urban flooding reduction: A community scale study. *Ecological Modelling, 291*, 6–14.

Liu, Z., Cai, Y., Wang, S., Lan, F., & Wu, X. (2020). Small and medium-scale river flood controls in highly urbanized areas: A whole region perspective. *Water, 12*(1), 182. https://doi.org/10.3390/w12010182

Liu, Z., Xu, C., Xu, T., Jia, H., Zhang, X., Chen, Z., & Yin, D. (2021). Integrating socioecological indexes in multiobjective intelligent optimization of green-grey coupled infrastructures. *Resources, Conservation and Recycling, 174*, Article 105801. https://doi.org/10.1016/j.resconrec.2021.105801

Lu, P., & Sun, Y. (2021). Scenario-based hydrodynamic simulation of adaptive strategies for urban design to improve flood resilience: A case study of the Mingzhu Bay Region, Guangzhou, Greater Bay Area. *River Research and Applications*. doi:10.1002/rra.3913.

Matthews, J. C. (2016). Disaster resilience of critical water infrastructure systems. *Journal of Structural Engineering, 142*(8), C6015001.

Meyer, H., & Nijhuis, S. (2013). Delta urbanism: Planning and design in urbanized deltas – Comparing the Dutch delta with the Mississippi River delta. *Journal of Urbanism: International Research on Placemaking and Urban Sustainability, 6*(2), 160–191. https://doi.org/10.1080/17549175.2013.820210

Mishra, D., & Satapathy, S. (2020). MCDM approach for mitigation of flooding risks in Odisha (India) based on information retrieval. *International Journal of Cognitive Informatics and Natural Intelligence (IJCINI), 2*, 77–91. https://doi.org/10.4018/IJCINI.2020040105

Mulliner, E., Malys, N., & Maliene, V. (2016). Comparative analysis of MCDM methods for the assessment of sustainable housing affordability. *Omega, 59*, 146–156. https://doi.org/10.1016/j.omega.2015.05.013

Neal, J., Schumann, G., Fewtrell, T., Budimir, M., Bates, P., & Mason, D. (2011). Evaluating a new LISFLOOD-FP formulation with data from the summer 2007 floods in Tewkesbury, UK. *Journal of Flood Risk Management, 4*(2), 88–95. https://doi.org/10.1111/j.1753-318X.2011.01093.x

O'Donnell, E., Thorne, C., Ahilan, S., Arthur, S., Birkinshaw, S., Butler, D., … Wright, N. (2020). The blue-green path to urban flood resilience. *Blue-Green Systems, 2*(1), 28–45. https://doi.org/10.2166/bgs.2019.199

Olson, D. L. (2004). Comparison of weights in TOPSIS models. *Mathematical and Computer Modelling, 40*(7–8), 721–727.

Patro, S., Chatterjee, C., Mohanty, S., Singh, R., & Raghuwanshi, N. S. (2009). Flood inundation modeling using MIKE FLOOD and remote sensing data. *Journal of the Indian Society of Remote Sensing, 37*(1), 107–118. https://doi.org/10.1007/s12524-009-0002-1

Prinsen, G. F., & Becker, B. P. (2011). Application of SOBEK hydraulic surface water models in the Netherlands Hydrological Modelling Instrument. *Irrigation and Drainage, 60*, 35–41. https://doi.org/10.1002/ird.665

Pugliese, F., Gerundo, C., Paola, F. D., Caroppi, G., & Giugni, M. (2022). Enhancing the urban resilience to flood risk through a decision support tool for the LID-BMPs optimal design. *Water Resources Management, 36*, 5633–5654.

Shishegar, S., Duchesne, S., & Pelletier, G. (2018). Optimization methods applied to stormwater management problems: A review. *Urban Water Journal, 15*(3), 276–286. https://doi.org/10.1080/1573062X.2018.1439976

Sidek, L. M., Jaafar, A. S., Majid, W. H., Basri, H., Marufuzzaman, M., Fared, M. M., & Moon, W. C. (2021). High-resolution hydrological-hydraulic modeling of urban floods using InfoWorks ICM. *Sustainability, 13*(18), 10259. https://doi.org/10.3390/su131810259

Tavakol-Davani, H., Burian, S. J., Devkota, J., & Apul, D. (2016). Performance and cost-based comparison of green and gray infrastructure to control combined sewer overflows. *Journal of Sustainable Water in the Built Environment, 2*(2), 04015009. https://doi.org/10.1061/JSWBAY.0000805

Watróbski, J., Baczkiewicz, A., Ziemba, E., & Sałabun, W. (2020). Temporal VIKOR - A New MCDA Method Supporting Sustainability Assessment. Retrieved from https://aisel.aisnet.org/isd2014/proceedings2022/usability/7/.

Xu, C., Liu, Z., Chen, Z., Zhu, Y., Yin, D., Leng, L., … Fu, G. (2021). Environmental and economic benefit comparison between coupled grey-green infrastructure system and traditional grey one through a life cycle perspective. *Resources, Conservation and Recycling, 174*, Article 105804. https://doi.org/10.1016/j.resconrec.2021.105804

Yang, G., & Best, E. P. (2015). Spatial optimization of watershed management practices for nitrogen load reduction using a modeling-optimization framework. *Journal of*

Environmental Management, 161, 252–260. https://doi.org/10.1016/j.jenvman.2015.06.052

Yin, D., Chen, Y., Jia, H., Wang, Q., Chen, Z., Xu, C., … Chen, A. S. (2021). Sponge city practice in China: A review of construction, assessment, operational and maintenance. *Journal of Cleaner Production, 280*, Article 124963. https://doi.org/10.1016/j.jclepro.2020.124963

Yin, D., Evans, B., Wang, Q., Chen, Z., Jia, H., Chen, A. S., … Leng, L. (2020). Integrated 1D and 2D model for better assessing runoff quantity control of low impact development facilities on community scale. *Science of The Total Environment, 730*, Article 137630. https://doi.org/10.1016/j.scitotenv.2020.137630

Yin, D., Xu, C., Jia, H., Yang, Y., Sun, C., Wang, Q., & Liu, S. (2022). Sponge city practices in China: From pilot exploration to systemic demonstration. *Water, 14*(10), 1531. https://doi.org/10.3390/w14101531

Zhang, C., Wang, Y., Li, Y., & Ding, W. (2017). Vulnerability analysis of urban drainage systems: Tree vs. loop Networks. *Sustainability, 9*(3), 397.

Zhang, X., Lin, R., Huirong, X., & Wang, X. (2019). Simulation study on urban waterlogging in Donghao River drainage area in Guangzhou based on MIKE URBAN. *Pearl River, 40*(7), 12–17. https://doi.org/10.3969/j.issn.1001-9235.2019.07.003

Zhang, Z., Meng, F., Zeng, Y., Liu, J., Yuan, D., Fong, S., & Yang, L. (2021). Identification of Urban Rainstorm Waterlogging Based on Multisource Information Fusion: A Case Study in Futian District, Shenzhen. In *E3S Web of Conferences. 259* (p. 01004). EDP Sciences.

Zhu, Y., Tian, D., & Yan, F. (2020). Effectiveness of entropy weight method in decision-making. *Mathematical Problems in Engineering, 2020*. https://doi.org/10.1155/2020/3564835